

Title	Defect Termination of Flash-Lamp-Crystallized Large-Grain Polycrystalline Silicon Films by High-Pressure Water Vapor Annealing
Author(s)	Ohdaira, Keisuke
Citation	Japanese Journal of Applied Physics, 52(4): 04CR11-1-04CR11-4
Issue Date	2013-04-22
Type	Journal Article
Text version	author
URL	http://hdl.handle.net/10119/11393
Rights	This is the author's version of the work. It is posted here by permission of The Japan Society of Applied Physics. Copyright (C) 2013 The Japan Society of Applied Physics. Keisuke Ohdaira, Japanese Journal of Applied Physics, 52(4), 2013, 04CR11. http://jjap.jsap.jp/link?JJAP/52/04CR11/
Description	

Defect Termination of Flash-Lamp-Crystallized Large-Grain Polycrystalline Silicon Films by High-Pressure Water Vapor Annealing

Keisuke Ohdaira^{1,2}

¹Japan Advanced Institute of Science and Technology (JAIST),

Nomi, Ishikawa 923-1292, Japan

²PRESTO, Japan Science and Technology Agency (JST),

Kawaguchi, Saitama 332-0012, Japan

E-mail: ohdaira@jaist.ac.jp

High-pressure water-vapor annealing (HPWVA) is performed on 3- μ m-thick polycrystalline silicon (poly-Si) films formed on glass substrates by crystallizing electron-beam (EB)-evaporated precursor amorphous Si (a-Si) films by flash lamp annealing (FLA). HPWVA at higher temperature and pressure tends to result in a lower defect density of FLC poly-Si films. The defect density of FLC poly-Si films can be reduced from $\sim 3 \times 10^{17}$ to $\sim 2 \times 10^{16}$ /cm³ when the HPWVA temperature is 500 °C and the pressure is more than 8 MPa, which is sufficiently of device grade. The annealing of flash-lamp-crystallized (FLC) poly-Si films under inert-gas atmosphere does not lead to sufficient reduction in their defect density, indicating the necessity of water vapor during annealing.

1. Introduction

Thin-film polycrystalline silicon (poly-Si) has attracted considerable interest as a photovoltaic material because of the low amount of Si usage and its high stability against light soaking. The crystallization of precursor amorphous Si (a-Si) films prepared on low-cost substrates through annealing process is one of the most promising approaches to obtaining poly-Si films.¹⁻⁴⁾ Of a variety of annealing techniques, we have investigated flash lamp annealing (FLA), i.e. millisecond-order discharge from Xe lamps.⁵⁻⁸⁾ Owing to its appropriate annealing duration,⁹⁻¹⁰⁾ a single shot of a flash pulse can crystallize μm -order-thick a-Si films without serious thermal damage to glass substrates. We have so far confirmed that more than 4 μm thick poly-Si films can be formed on glass substrates by FLA.⁵⁻⁸⁾ The crystallization induced by FLA is based on explosive crystallization (EC), lateral crystallization driven by the release of latent heat. We have observed various types of ECs,^{7,8)} and EC governed by liquid-phase epitaxy (LPE) occurs particularly when electron-beam (EB)-evaporated a-Si films are used as precursors, resulting in the formation of poly-Si films with relatively large grains.^{11,12)} Unlike flash-lamp-crystallized (FLC) poly-Si films formed from chemical-vapor-deposited (CVD) hydrogenated a-Si films,¹³⁾ FLC poly-Si films formed from EB-evaporated a-Si films are expected to contain few hydrogen atoms; thus, effective defect termination is required to obtain FLC poly-Si films with a low defect density.

In this study, we have performed high-pressure water-vapor annealing (HPWVA) on FLC poly-Si films formed from EB-evaporated a-Si films. HPWVA is a defect-terminating annealing technique developed by Sameshima and Satoh, in which samples are heated in a high-pressure water vapor atmosphere.¹⁴⁾ The effectiveness of

HPWVA for the defect termination of thin (<100 nm) poly-Si films has been well confirmed.¹⁵⁾ Our aim to apply HPWVA is to reduce the defect density of thick (>1 μm) poly-Si films for solar cell application. Although we have already reported the application of HPWVA to μm -order-thick FLC poly-Si films,¹⁶⁾ the FLC poly-Si films obtained contain a number of hydrogen atoms since their precursor is hydrogenated catalytic CVD (Cat-CVD) a-Si films. Note that the improvement in the properties of poly-Si films could be due to defect termination by hydrogen atoms during HPWVA. Here, we used unhydrogenated a-Si precursor films and their resulting FLC poly-Si films with a much less smaller number of hydrogen atoms, and clearly show the effectiveness of HPWVA on thick poly-Si films. The advantage of using EB-evaporated a-Si precursor films is the formation of poly-Si films with much larger grains, several tens of μm long along EC directions,^{11,12)} than the case of Cat-CVD a-Si films, containing 10-nm-sized fine grains.⁷⁾ This can contribute to the realization of solar cells with better performance if their defects are well terminated.

2. Experimental Procedure

3- μm -thick intrinsic a-Si films were deposited by EB evaporation directly on $20\times 20\times 0.7\text{ mm}^3$ quartz glass substrates heated at 200 °C at a deposition rate of 250 nm/min at a pressure of $4.2\times 10^{-4}\text{ Pa}$. The hydrogen content of the EB-evaporated a-Si films was evaluated by secondary-ion mass spectrometry (SIMS). We then performed FLA on each sample at a fluence of $\sim 15\text{ J/cm}^2$ and a stage heating temperature of 500 °C under Ar atmosphere using a FLA system manufactured by Design System. A Xe lamp equipped in the FLA system was produced by ORC Manufacturing. Only one shot of flash irradiation was given for each sample. The spectrum of the flash lamp

light used in this study is shown in Fig. 1. Details of the FLA system used in this study has been summarized elsewhere.⁸⁾ The crystallization and crystalline fraction of Si films after FLA were characterized by Raman spectroscopy using a He-Ne laser with a wavelength of 632.8 nm.

HPWVA was performed on the FLC poly-Si films after cutting to small pieces with a size of roughly $2 \times 10 \text{ mm}^2$. Figure 2 shows the appearance of the HPWVA chamber used in this study. A poly-Si sample and about 15 g of deionized water were placed in a cylindrical space with a diameter of 41 mm and a height of 25 mm. The chamber was then sealed using a Au-coated Cu gasket. Treatment pressure was changed up to $\sim 26 \text{ MPa}$ using a relief valve that serves to release excess water vapor when chamber pressure exceeds a setting value. After covering the chamber with a thermal insulator, it was heated with heaters embedded in the upper and lower blocks up to a setting value ($350\text{-}500 \text{ }^\circ\text{C}$) for 3 h, and kept at temperature for another 3 h. Heating is then stopped heating and the thermal insulator is removed to cool the chamber. For comparison, we also performed the furnace annealing of FLC poly-Si films at $350\text{-}500 \text{ }^\circ\text{C}$ in Ar atmosphere for 3 h, and rapid thermal annealing (RTA) in Ar atmosphere for 3 min at $900\text{-}1050 \text{ }^\circ\text{C}$, which is generally referred to as “defect annealing”.^{17,18)} The number of dangling bonds in the FLC poly-Si films before and after HPWVA was determined by electron spin resonance (ESR), and its density was calculated by dividing the number of dangling bonds by the volume of FLC poly-Si. The defect density of the precursor EB-evaporated a-Si is $\sim 2 \times 10^{19} / \text{cm}^3$.

3. Results and Discussion

Figure 3 shows the SIMS profile of hydrogen atoms in a precursor EB-evaporated

a-Si film. Only a small amount of hydrogen on the order of 10^{19} /cm³ is incorporated in the a-Si film, which is two orders of magnitude lower than that in hydrogenated Cat-CVD a-Si films.¹³⁾ We thus cannot expect effective defect termination by hydrogen atoms remaining in Si films. Note that the difference between hydrogen contents of the Cat-CVD and EB-evaporated a-Si films is not the reason for the considerable grain size difference. This is because the use of sputtered a-Si films, with no intentional hydrogen inclusion, leads to the emergence of EC similarly to the case of Cat-CVD precursor a-Si films and the resulting formation of 10-nm-sized fine grains.¹⁹⁾

Figure 4 shows a typical Raman spectrum of a FLC poly-Si film formed from an EB-evaporated a-Si film. A clear peak located at ~ 520 cm⁻¹ originating from the crystalline Si (c-Si) phase is observed, with no signal from a-Si phase at approximately 480 cm⁻¹. This indicates that poly-Si with a high crystalline fraction is formed by a single shot of a flash pulse. The position of the c-Si Raman peak of ~ 517 cm⁻¹ is lower than that in the case of FLC poly-Si films formed from Cat-CVD a-Si films, which have a c-Si peak at 520.5 cm⁻¹. This is due to the difference in film stress between the precursor a-Si films. EB-evaporated a-Si films originally have tensile stress, which remains even after crystallization.⁸⁾ The width of the c-Si peak in the Raman spectrum of a FLC poly-Si film formed from an EB-evaporated a-Si film is ~ 4.5 cm⁻¹. This is much smaller than that of FLC poly-Si films formed from Cat-CVD a-Si films, i.e., ~ 7 cm⁻¹.⁸⁾ This indicates a large difference in grain size between the two kinds of poly-Si films.^{5-8,11,12)} Note that we have observed no significant change in the width of the c-Si peaks of the FLC poly-Si films formed from EB-evaporated a-Si films even after furnace annealing, RTA, or HPWVA.

Figure 5(a) shows the defect density of the FLC poly-Si films before and after

furnace annealing under Ar atmosphere as a function of furnace annealing temperature. The defect density of an as-crystallized FLC poly-Si films is $\sim 3 \times 10^{17} / \text{cm}^3$, which is lower than that of excimer-laser-crystallized poly-Si films of $\sim 1 \times 10^{18} / \text{cm}^3$,¹⁵⁾ and similar to that of FLC poly-Si films containing a number of H atoms formed from hydrogenated Cat-CVD a-Si of $\sim 1 \times 10^{17} / \text{cm}^3$. This low defect density is probably due to the formation of large grains through LPE-based EC and the resulting smaller number of grain boundaries.^{11,12)} Even after annealing at up to 500 °C in Ar atmosphere, no reduction in the defect density is confirmed. This clearly indicates that the rearrangement of Si atoms to reduce dangling bonds does not effectively occur in this temperature range and that the supply of species for terminating Si dangling bonds from the outside is necessary. Figure 5(b) shows the defect densities of the FLC poly-Si films before and after RTA under Ar atmosphere as a function of RTA temperature. Although a slight decrease in defect density is observed after RTA at 1000-1050 °C, the effect of defect annealing by RTA on reducing the defect density of FLC poly-Si films seems insignificant. Since defect annealing is considered to reduce the density of point defects in poly-Si films,¹⁷⁾ this result might suggest that most dangling bonds exist at grain boundaries.

Figure 6 shows the defect density of the FLC poly-Si films before and after HPWVA at a constant pressure of ~ 1 MPa as a function of annealing temperature. As HPWVA temperature increases, the defect density of the poly-Si films decreases monotonically, and reaches $\sim 1 \times 10^{17} / \text{cm}^3$ at an annealing temperature of 500 °C. Since the defect density of poly-Si films after annealing in Ar at the same temperature is unchanged, as shown in Fig. 5(a), the decrease in defect density is considered to be the effect of high-pressure water vapor. The tendency of poly-Si films to show a lower

defect density at a higher HPWVA temperature has also been reported.¹⁵⁾ Figure 7 shows the defect density of the FLC poly-Si films before and after HPWVA at a constant temperature of 500 °C as a function of annealing pressure. The defect density of the FLC poly-Si films decreases more significantly with increasing water vapor pressure. The minimum defect density of a FLC poly-Si film obtained in this study is as low as $\sim 2 \times 10^{16} / \text{cm}^3$.

According to Asada *et al.*, the defect density of excimer-laser-crystallized poly-Si films can be decreased from $\sim 1 \times 10^{18}$ to $\sim 1 \times 10^{17} / \text{cm}^3$ after HPWVA at a pressure of 1.3 MPa at 310 °C for 3 h. The effect of HPWVA on FLC poly-Si films under similar HPWVA conditions is less significant, as shown in Fig. 6. Since the reported average grain size of poly-Si films formed by ELA is 45 nm,¹⁵⁾ H₂O molecules can diffuse more easily through grain boundaries in poly-Si films formed by ELA, which is one possible reason for the difference in HPWVA effect. Another likely reason for the difference is large difference in poly-Si film thickness: 50 nm for excimer-laser-crystallized poly-Si films and 3 μm for FLC poly-Si films. Higher pressure might be necessary to allow H₂O molecules to more deeply penetrate into poly-Si films. When we decrease HPWVA duration from 3 h to 5 min at ~ 8 MPa, the reduction in the defect density of the FLC poly-Si film becomes insufficient ($\sim 1.5 \times 10^{17} / \text{cm}^3$). This is probably due to the shorter diffusion time for H₂O molecules, indicating the importance of H₂O diffusion.

The defect density obtained in this study is much lower than that of FLC poly-Si films formed from hydrogenated Cat-CVD a-Si films, i.e., $\sim 5 \times 10^{16} / \text{cm}^3$, after furnace annealing under N₂ atmosphere.²⁰⁾ This might also be due to the difference in grain size. We have succeeded in obtaining 3- μm -thick poly-Si films with a low defect density equivalent to that of device-grade CVD a-Si and/or microcrystalline Si ($\mu\text{c-Si}$)

films. In particular, CVD μ c-Si films with a higher crystalline fraction generally tends to have more defects owing to the smaller amount of a-Si tissue surrounding crystalline grains.²¹⁾ In contrast, FLC poly-Si films formed in this study can combine the advantages of low defect density and lack of an a-Si tissue, and are thus thought to be a more promising material for photovoltaic application. The quality of the FLC poly-Si should also be compared to conventional bulk multicrystalline Si, which would be clarified by lifetime measurement. This necessitates further investigation.

4. Summary

HPWVA is effective for reducing the defect density of 3- μ m-thick FLC poly-Si films with large grains formed from EB-evaporated a-Si films. Higher HPWVA temperature and pressure result in a more effective defect termination of FLC poly-Si films. A similar result cannot be obtained by furnace annealing or RTA under Ar atmosphere. It is thus confirmed that the reduction in the defect density of FLC poly-Si films is attributed to water vapor. The defect density of FLC poly-Si films can be decreased from $\sim 3 \times 10^{17} / \text{cm}^3$ to as low as $\sim 2 \times 10^{16} / \text{cm}^3$. This value is of device grade, and thus FLC poly-Si films after HPWVA are a promising material for photovoltaic application.

Acknowledgments

The author would like to thank ULVAC Inc. for the preparation of the EB-evaporated a-Si films and L. Yang and S. Terashima of JAIST for their support in the experiments. This work was supported by JST PRESTO program.

- 1) T. Matsuyama, M. Tanaka, S. Tsuda, S. Nakano, and Y. Kuwano: Jpn. J. Appl. Phys. **32** (1993) 3720.
- 2) M. J. Keevers, T. L. Young, U. Schubert, and M. A Green: Proc. 22nd European Photovoltaic Solar Energy Conf., 2007, p. 1783
- 3) J. K. Saha, K. Haruta, M. Yeo, T. Koabayshi, and H. Shirai: Sol. Energy Mater. Sol. Cells **93** (2009) 1154.
- 4) S. Janz, S. Reber, H. Habenicht, H. Lautenschlager, and C. Schetter: Conf. Rec. 4th World Conf. Photovoltaic Energy Conversion (WCPEC), 2006, p. 1403
- 5) K. Ohdaira, Y. Endo, T. Fujiwara, S. Nishizaki, and H. Matsumura: Jpn. J. Appl. Phys. **46** (2007) 7603.
- 6) K. Ohdaira, T. Fujiwara, Y. Endo, S. Nishizaki, and H. Matsumura: Jpn. J. Appl. Phys. **47** (2008) 8239.
- 7) K. Ohdaira, T. Fujiwara, Y. Endo, S. Nishizaki, and H. Matsumura: J. Appl. Phys. **106** (2009) 044907.
- 8) K. Ohdaira, N. Tomura, S. Ishii, and H. Matsumura: Electrochem. Solid-State Lett. **14** (2011) H372.
- 9) B. Pécz, L. Dobos, D. Panknin, W. Skorupa, C. Lioutas, and N. Vouroutzis: Appl. Surf. Sci. **242** (2005) 185.
- 10) M. Smith, R. McMahon, M. Voelskow, D. Panknin, and W. Skorupa: J. Cryst. Growth **285** (2005) 249.
- 11) K. Ohdaira and H. Matsumura: J. Cryst. Growth **362** (2013) 149.
- 12) K. Ohdaira, K. Sawada, N. Usami, S. Varlamov, and H. Matsumura: Jpn. J. Appl. Phys. **51** (2012) 10NB15.

- 13) K. Ohdaira, H. Takemoto, K. Shiba, and H. Matsumura: Appl. Phys. Express **2** (2009) 061201.
- 14) T. Sameshima and M. Satoh: Jpn. J. Appl. Phys. **36** (1997) L687.
- 15) K. Asada, K. Sakamoto, T. Watanabe, T. Sameshima, and S. Higashi: Jpn. J. Appl. Phys. **39** (2000) 3883.
- 16) Y. Endo, T. Fujiwara, K. Ohdaira, S. Nishizaki, K. Nishioka, and H. Matsumura: Thin Solid Films **518** (2010) 5003.
- 17) M. L. Terry, A. Straub, D. Inns, D. Song, and A. G. Aberle: Appl. Phys. Lett. **86** (2005) 172108.
- 18) C. Becker, T. Sontheimer, S. Steffens, S. Scherf, and B. Rech: Energy Procedia **10** (2011) 61.
- 19) K. Ohdaira, S. Ishii, N. Tomura, and H. Matsumura: J. Nanosci. Nanotechnol. **12** (2012) 591.
- 20) K. Ohdaira, T. Nishikawa, S. Ishii, N. Tomura, K. Koyama, and H. Matsumura: Proc. 5th World Conf. Photovoltaic Energy Conversion, 2010, p. 3546.
- 21) A. L. B. Neto, T. Dylla, S. Klein, T. Repmann, A. Lambertz, R. Carius, and F. Finger: J. Non-Cryst. Solids **338–340** (2004) 168.

Figure captions

Fig. 1 Spectrum of Xe flash lamp light used in this study.

Fig. 2 Appearance of HPWVA chamber used in this study.

Fig. 3 SIMS profile of hydrogen atoms in EB-evaporated a-Si film.

Fig. 4 Raman spectrum of a FLC poly-Si film formed from an EB-evaporated a-Si film. The spectrum of a c-Si wafer is also shown for comparison.

Fig. 5 Defect density of FLC poly-Si films as functions of (a) furnace annealing temperature and (b) RTA temperature. The dashed lines are guides to the eye.

Fig. 6 Defect density of FLC poly-Si films as a function of HPWVA temperature at constant pressure of ~ 1 MPa. Dashed line is a guide to the eye.

Fig. 7 Defect density of FLC poly-Si films as a function of HPWVA pressure at constant temperature of $500\text{ }^{\circ}\text{C}$. A dashed line is a guide to the eye.

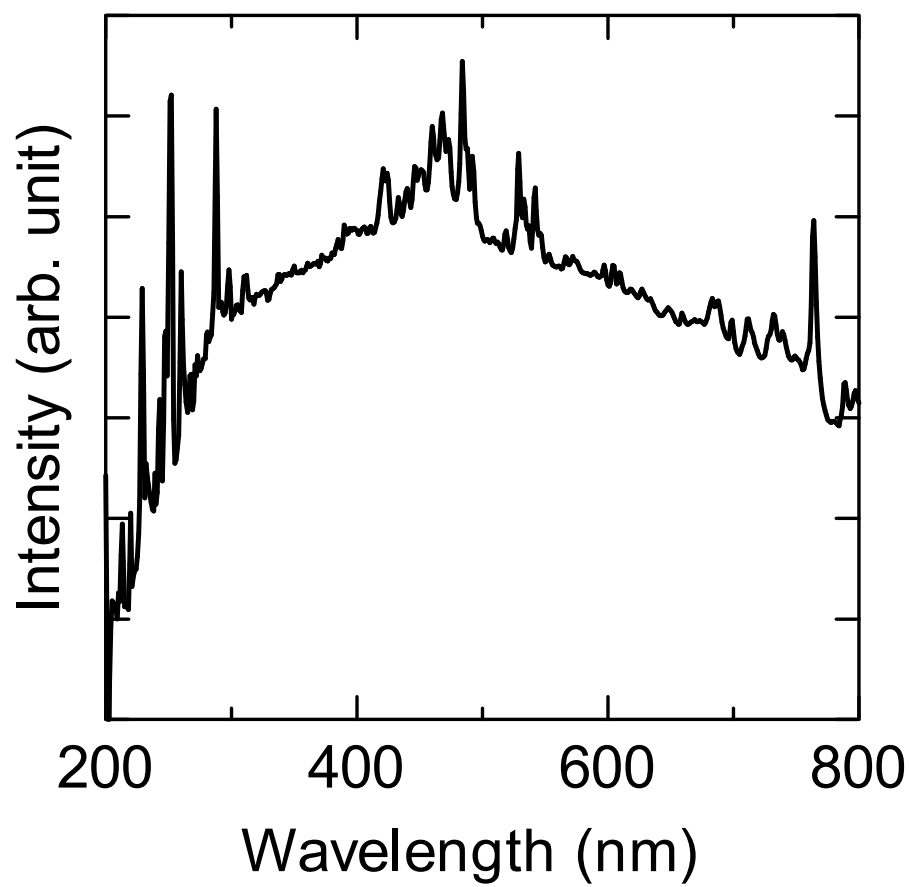


Figure 1 K. Ohdaira

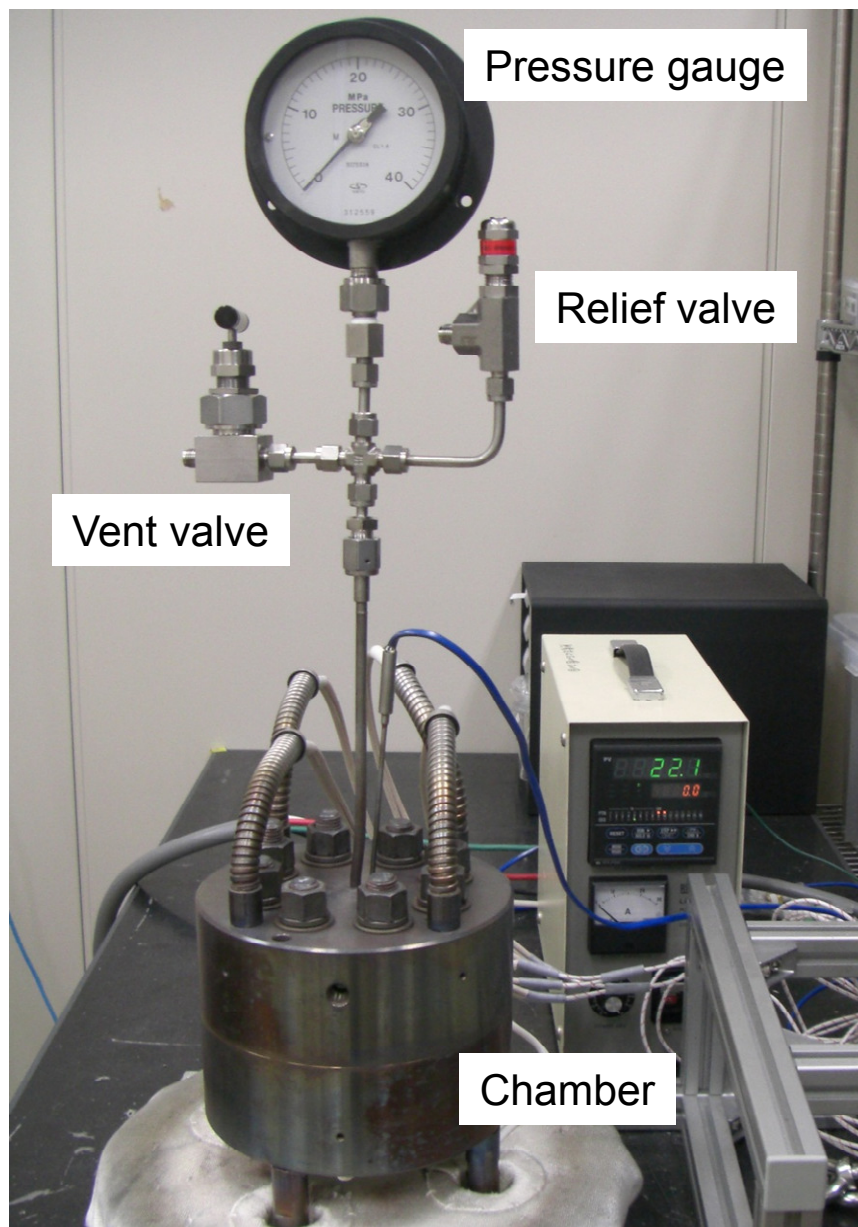


Figure 2 K. Ohdaira

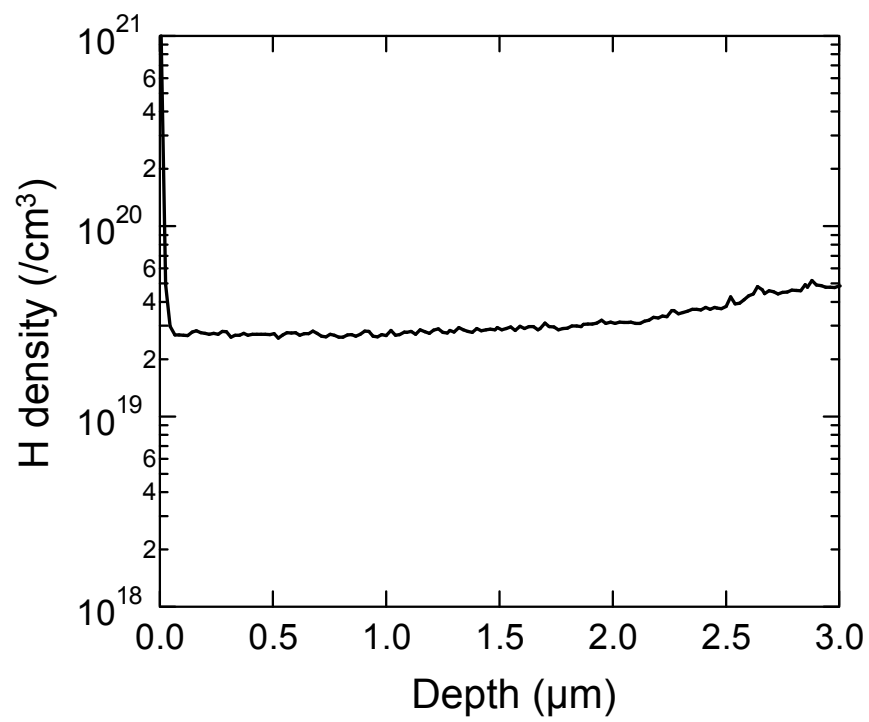


Figure 3 K. Ohdaira

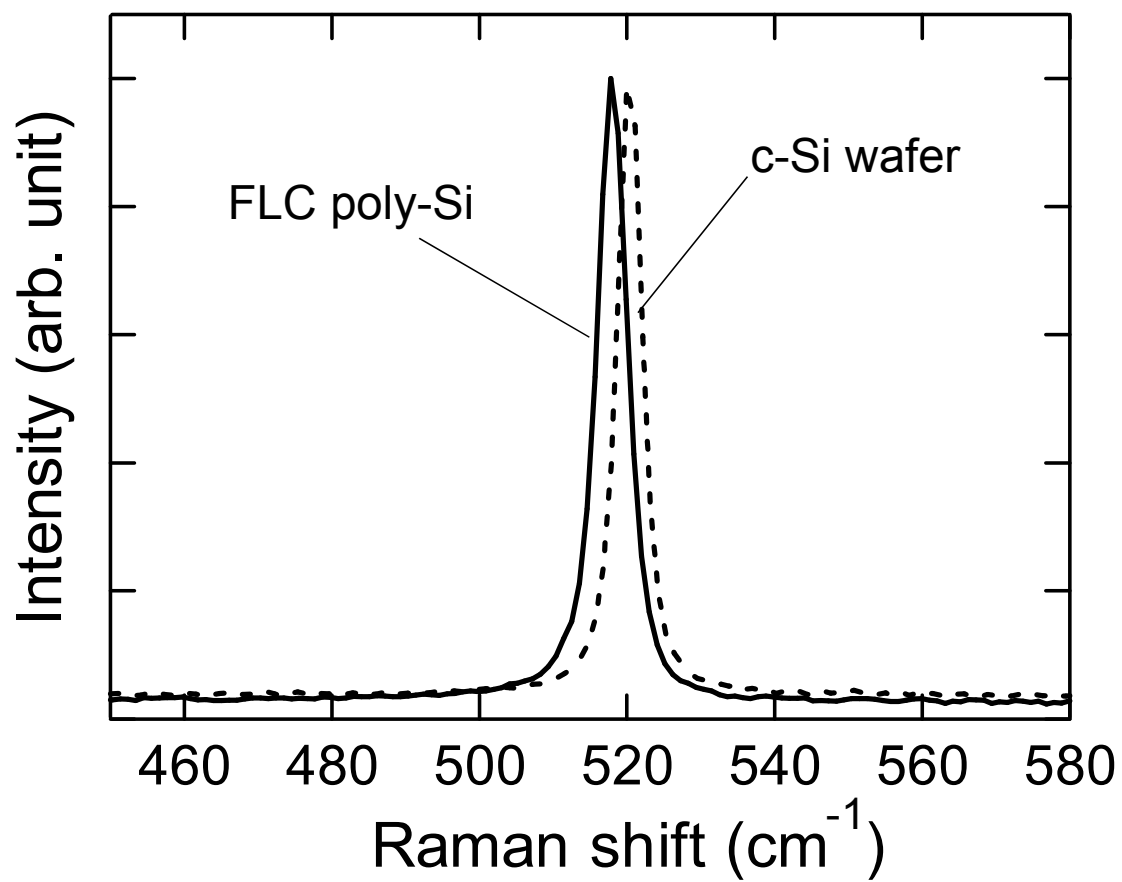


Figure 4 K. Ohdaira

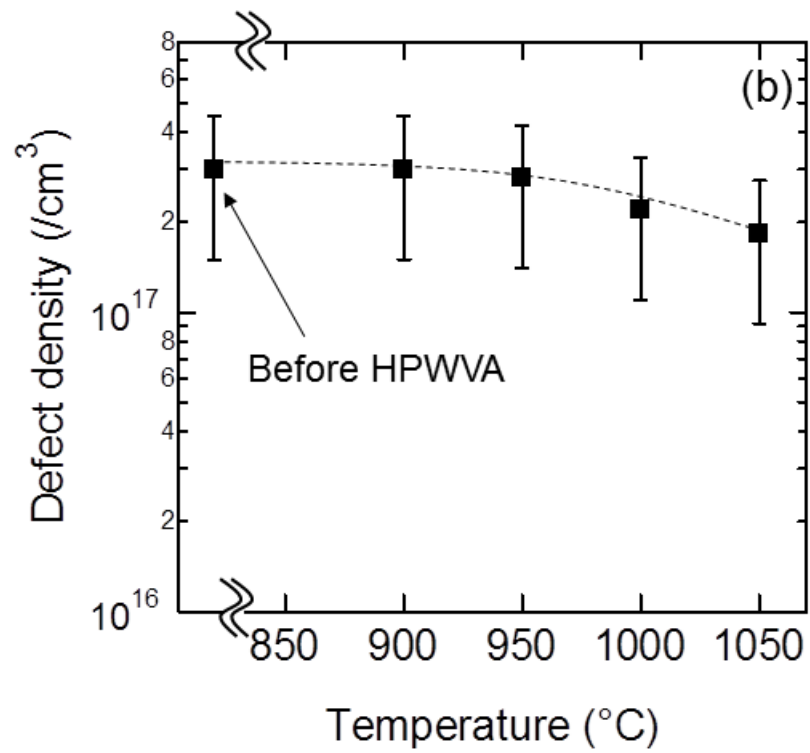
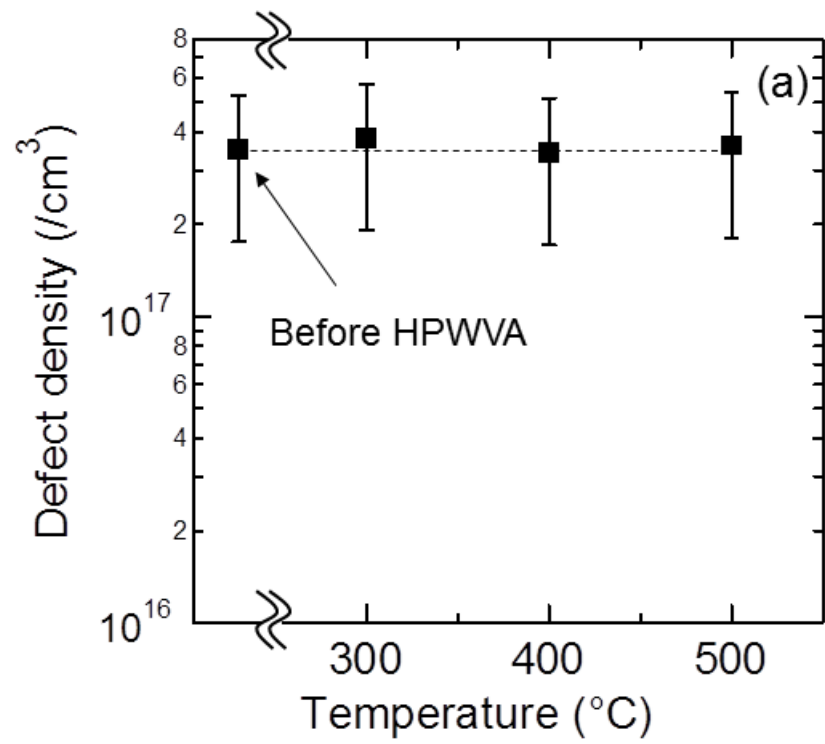


Figure 5 K. Ohdaira

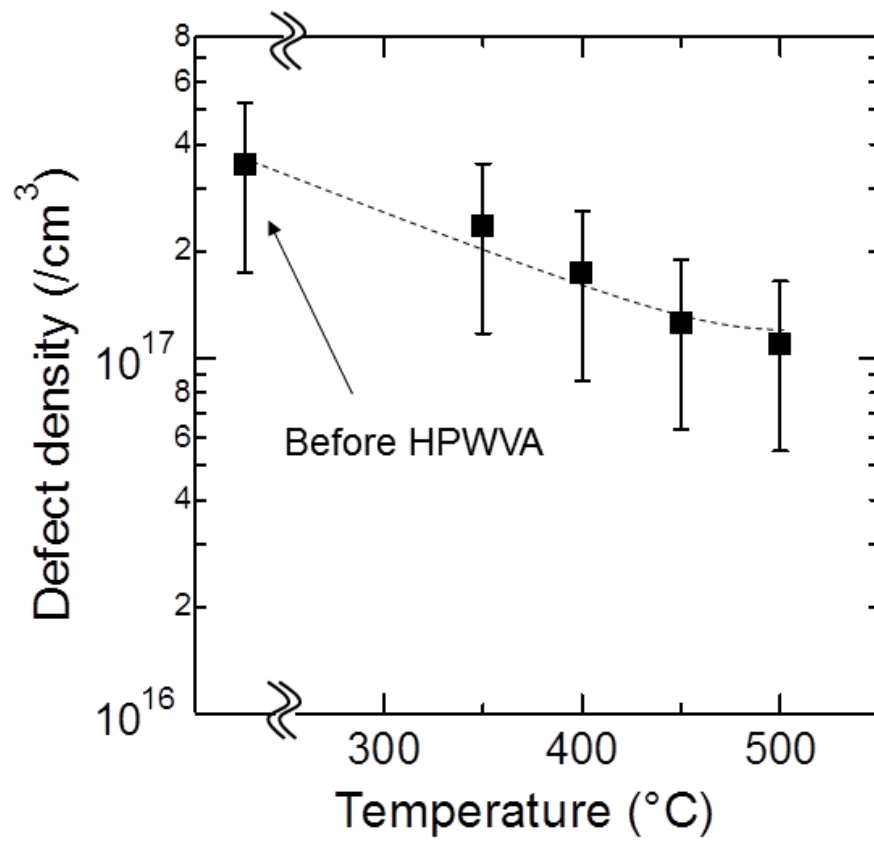


Figure 6 K. Ohdaira

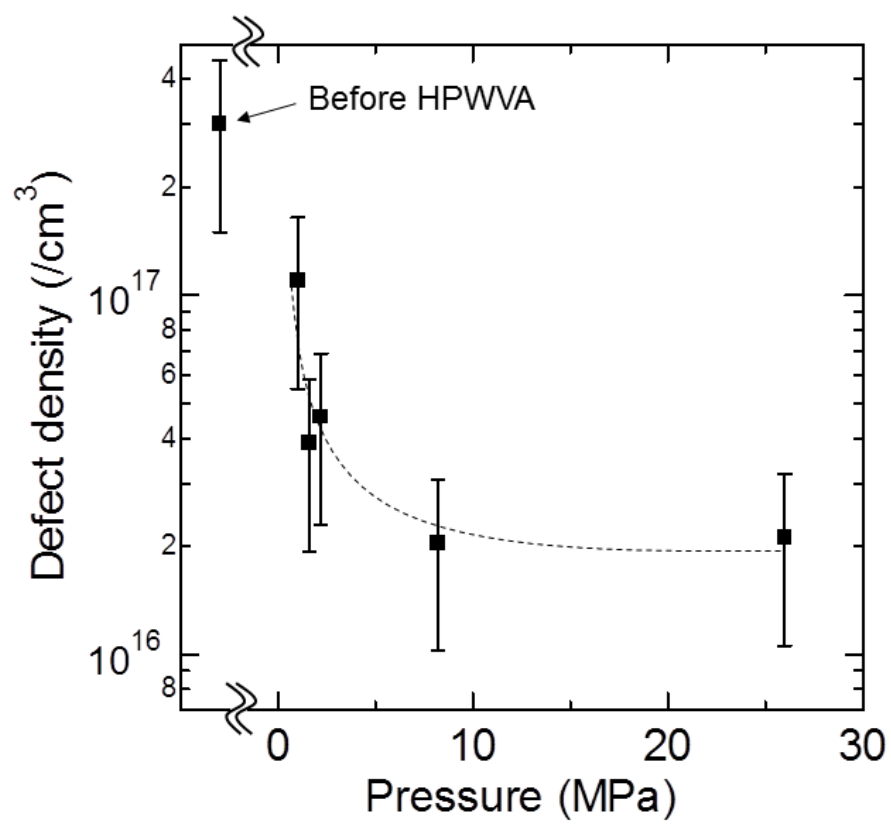


Figure 7 K. Ohdaira